J Radioanal Nucl Chem (2016) 307:835–842
DOI 10.1007/s10967-015-4283-2

X-ray diffraction, spectral, thermal and surface morphological studies of gamma-irradiated diaquamalonatomanganese(II) (DMM)

I. S. Sumithra[1] · T. A. Jayashri[1] · G. Krishnan[2]

Received: 11 February 2015 / Published online: 17 July 2015

Abstract The effect of gamma irradiation on single crystal and powdered samples of diaquamalonatomanganese(II) was investigated. Thermal, spectral and surface morphological studies were also performed using the powdered samples before and after irradiation. Single crystal as well as PXRD studies showed that both unirradiated and irradiated samples are orthorhombic. Changes in lattice parameters upon irradiation are different in powder and single crystal of the same material. Thermal decomposition profiles of unirradiated and irradiated samples are found to be similar. Upon irradiation significant changes were observed in spectral features. AFM studies revealed morphological changes and enhanced roughness in the irradiated sample.

Keywords Irradiated malonato complexes · X-ray diffraction · Infrared spectra · Photoluminescence · Atomic force microscopy

Introduction

Solid state irradiation of molecular crystals leads to the production of lattice defects and chemical damage. Consequently any subsequently measured solid state property is found to be modified beneficially or not. The effects of gamma irradiation on various physicochemical properties have been investigated in a few inorganic salts, metal complexes, polymers and alloys [1–7]. Our previous studies on PXRD pattern of nickel amine complexes revealed that gamma irradiation leads to lattice distortion and significant changes in lattice parameters, relative intensity and crystallinity. The crystal system was found to be retained after irradiation [4, 5, 8, 9]. All these studies were performed with powdered samples of uniform mesh size. However studies concerning the effect of irradiation on crystal structure and crystallographic characteristics of single crystal and powdered samples of the same material have not been reported. Hence the present investigation focuses on single crystal and PXRD studies of the same material before and after gamma irradiation. We have selected diaquamalonatomanganese(II) (DMM) for this purpose as its single crystals can be easily grown by slow evaporation technique.

Thermal studies of irradiated nickel ammine complexes with different counter ions like nitrate, sulfate and oxalate have been reported from this laboratory [4, 5, 8, 9]. All these studies showed that pre-treatment leads to enhancement of thermal decomposition without changing the decomposition pattern. Effect of gamma irradiation on UV–Vis spectra of amine complexes of nickel and cobalt has been investigated. Results revealed that irradiation results in a change in the appearance of absorption peak whose intensity depends on the applied dose and nature of metal ions [2, 4, 5]. Fourier Transform Infrared (FT-IR) spectral studies of nickel amine complexes showed significant changes in position and intensity of characteristic bands after irradiation [8, 9]. Literature survey revealed that impact of irradiation on single crystals and subsequent changes in photoluminescence (PL) properties have been investigated [10, 11]. PL studies of pure and gamma

Electronic supplementary material The online version of this article (doi:10.1007/s10967-015-4283-2) contains supplementary material, which is available to authorized users.

✉ T. A. Jayashri
drjayashrita@yahoo.co.in

[1] Department of Chemistry, University of Kerala, Kariavattom, Thiruvananthapuram 695581, Kerala, India

[2] Department of Chemistry, University College, Thiruvananthapuram 695034, Kerala, India

irradiated L-alanine, single crystal showed that the PL intensity was enhanced upon irradiation. The enhancement was attributed to radical induced color centers favoring photoluminescence property of the compound [11]. The effect of gamma irradiation on the structure and photoluminescence properties of gallium based ferro spinel material in the powder form has also been investigated. It was found that gamma irradiation induced remarkable change in both structure and photoluminescence properties [12]. Recently we have reported surface morphological changes on gamma irradiated tris (1,2-diaminoethane) nickel(II) sulphate by SEM analysis. It was observed that surface morphological changes were produced by irradiation [9]. Hence the present investigation also proposes thermal, spectral (FT-IR, PL, and UV–Vis) and surface morphological studies by AFM before and after gamma irradiation of powdered DMM. Malonato complexes having metal organic frame works find numerous applications in crystal engineering, nano technology, catalysis, synthesis of new co-ordination polymers, and so on [13, 14]. Therefore, it is expected that knowledge regarding radiation damage and subsequently modified solid-state properties of such complexes would make substantial contributions in these fields.

Experimental

Preparation of DMM

Single crystals of DMM for the present investigation were grown by simple slow evaporation technique. Malonic acid (1 mmol) is added to an aqueous solution of manganese(II) acetate (2 mmol) under continuous stirring. The solution is heated on a water bath and the volume is reduced by half. The resulting solution is kept at room temperature for slow evaporation. Well shaped, shiny pink coloured crystals are obtained after 3 days. The crystals were washed with acetone and water and dried over P_2O_5. In order to get the powdered sample large crystals were ground and sieved to uniform mesh size.

Characterization

The prepared sample was characterized by elemental analysis, spectral and magnetic studies. The carbon and hydrogen contents in the obtained sample were determined by using Elementar Vario-EL 111 CHNS analyzer. The complex was found to have octahedral geometry.

Irradiation

Single crystals were encapsulated in glass ampoules. Similarly powdered samples of DMM sieved to uniform mesh size were also encapsulated in glass ampoules. They were exposed to ^{60}Co gamma ray up to 600 kGy in a Gamma chamber 560,000 cc self-shielded under room temperature at constant intensity at a dose rate of 6 kGy/h.

X-ray diffraction studies

Single crystal

Single crystal studies of unirradiated and sample irradiated to 600 kGy were performed. A well-shaped crystal of 0.30 × 0.25 × 0.20 mm was mounted on a Bruker AXS Kappa Apex2 CCD diffractometer with graphite monochromated Mo $K\alpha$ ($\lambda = 0.71073$ Å) radiation. The unit cell dimensions and intensity data were collected at 296 (±2) K. The structure was solved using SIR92 [15] and refinement was carried out by full-matrix least squares on F^2 using SHELXL-97 [16]. All non-hydrogen atoms were refined anisotropically. In the above complex the malonate hydrogen atoms were located from difference Fourier maps and refined with isotropic temperature factors. The final Fourier- difference map showed maximum and minimum height peaks of 0.254 and −0.297 e Å^{-3}. The final molecular graphics tool used was Diamond program [17]. The technical details of data acquisition and some selected refinement results such as selected bond lengths, bond angles and the hydrogen bonding interactions of irradiated DMM are provided in supplementary information file.

The following studies were carried out using powdered samples of DMM (unirradiated and sample irradiated to 600 kGy).

X-ray powder diffraction studies

The X-ray powder pattern were recoded using a Bruker AXS D8 advance XRD with Cu Kα radiation ($\lambda = 1.54056$ Å) in the range 2θ equal to 2°–80° adopting high score plus software for data processing. Goniometer radius is 240 mm.

Thermal studies

Non-isothermal studies were carried out in a Perkin Elmer STA 6000 model instrument in nitrogen atmosphere at a heating rate of 10 °C min^{-1}. The sample mass was kept constant around 3 ± 0.5 mg.

Spectral studies

FTIR spectra

The FT-IR spectra were recorded as Perkin Elmer infrared (IR) spectrophotometer in the range 3900–400 cm^{-1}.

Photoluminescence spectrum in solid state

Fluorescence spectra in solid state at room temperature were recorded on Flourolog III modular Spectroflourometer (Horiba Jobin–Yvon) equipped with 450 W Xenon lamp and Hamatsu R928-28 photomultiplier.

UV–visible spectrum in solid state

The electronic spectra were recorded on Schimadzhu UV-2450 UV–Vis spectrophotometer in the range 200–700 nm at room temperature.

AFM

The atomic force microscopic studies were carried out on Bruker Dimension Edge. In order to optimize the AFM measurements, the images were recorded on samples prepared by coating on a glass slide. AFM measurements of the prepared samples were performed in non-contacting mode.

Results and discussion

X-ray diffraction studies

X-ray crystallographic studies

The results of single crystal studies of irradiated DMM are presented in (Fig. 1). The asymmetric unit of irradiated DMM crystal is shown in (Fig. 2). The unirradiated sample had the same structure, the only difference being in the cell parameters (Table 1). Single crystal studies of DMM have already been reported [18]. In the present study also the system was found to be orthorhombic. Moreover irradiated sample retains the geometry, but the lattice parameters are found to be slightly changed.

X-ray powder diffraction

X-ray powder diffraction patterns of unirradiated and irradiated samples of DMM are given in (Fig. 3). Peak intensities, 2θ and d values are shown (Table 2). In the unirradiated sample the most intense peak arises from (101) plane, while in irradiated it is from (111) plane. In the irradiated sample an additional peak from (002) plane with increased intensity is observed. Position and intensity of the major peak is found to be slightly increased after irradiation. Additional peaks at different 2θ and d spacing values, with increased intensity are also observed in the irradiated sample. These peaks may be related to new phases produced due to irradiation. PXRD data were indexed using analytical

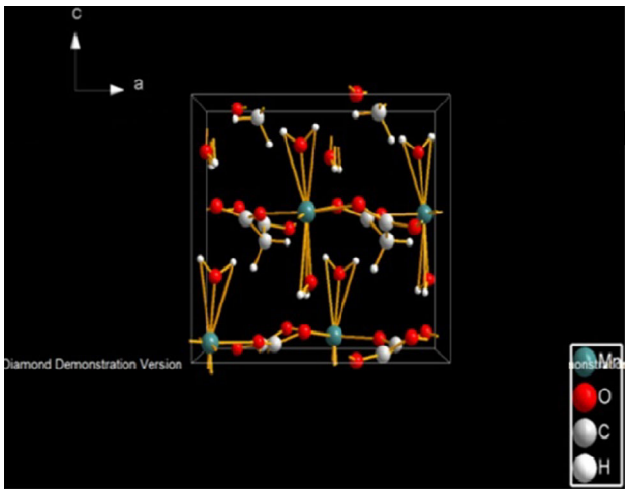

Fig. 1 Packing diagram of irradiated DMM viewed along the *b*-axis

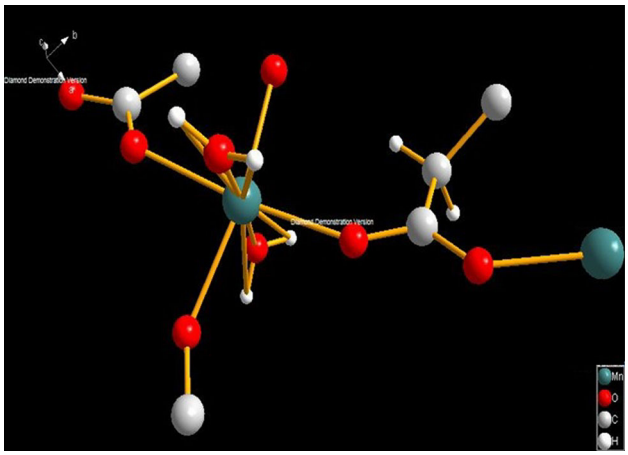

Fig. 2 Asymmetric unit of irradiated DMM

Table 1 Lattice parameters of unirradiated and irradiated DMM from single crystal studies

Unit cell	Unirradiated	Irradiated
a (Å)	9.618 (±0.009)	9.607 (4)
b (Å)	7.362 (±0.003)	7.364 (3)
c (Å)	8.322 (±0.003)	8.338 (3)
α (deg.)	90	90
β (deg.)	90	90
Υ (deg.)	90	90
V (Å^3)	589.3	589.8
Crystal system	Orthorhombic	Orthorhombic

methods developed by Lipson and Steeple [19]. Both the samples are found to be orthorhombic. The unit cell parameters, lattice constants, unit cell volume and density were evaluated. Average crystallite size was calculated using the Debye-Scherer formula [20]. The results are

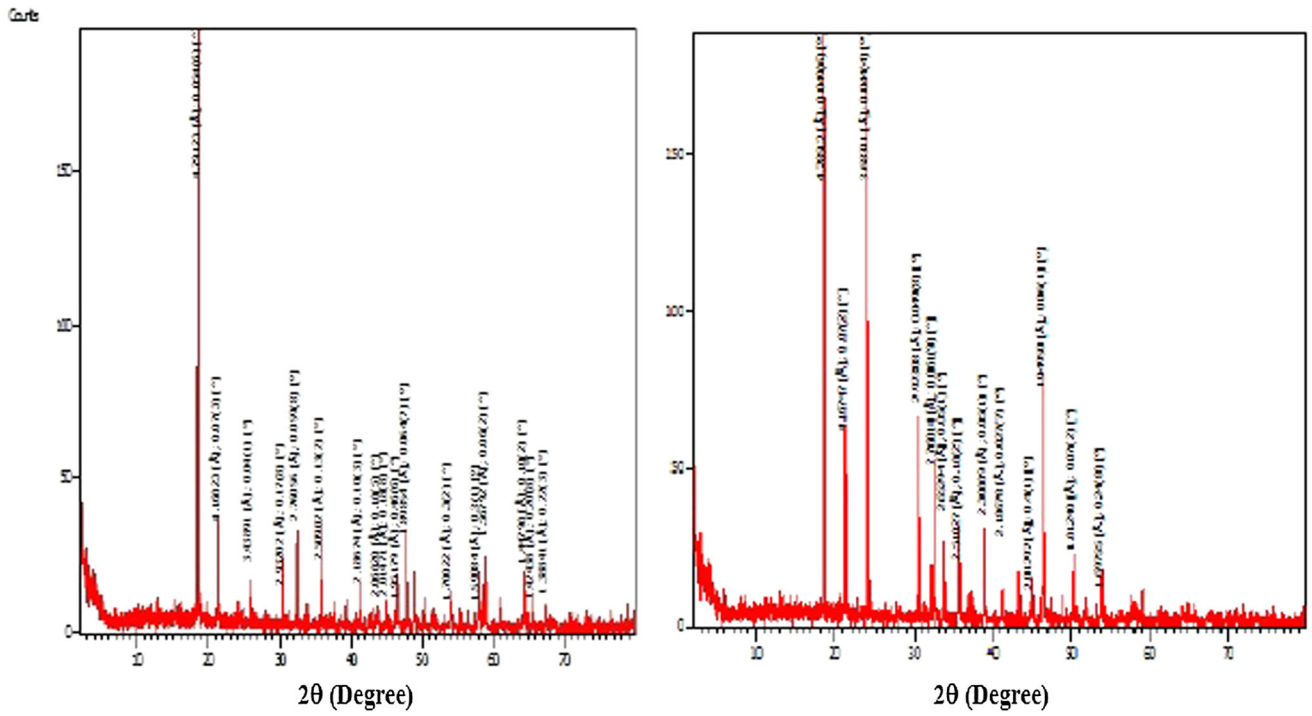

Fig. 3 PXRD pattern of unirradiated DMM (*left*) and irradiated DMM (*right*)

Table 2 X-ray powder diffraction data of unirradiated and irradiated DMM

Unirradiated				Irradiated			
2θ	*d*-spacing (Å)	hkl	Relative intensity (%)	2θ	*d*-spacing (Å)	hkl	Relative intensity (%)
18.504 (1)	4.79123	101	100	18.527 (1)	4.78512	111	100
21.299 (5)	4.16823	002	15.63	21.303 (3)	4.16747	020	29.58
25.888 (5)	3.43891	102	8.12	24.139 (1)	3.68391	002	94.33
30.46 (2)	2.93202	200	4.06	30.558 (2)	2.92308	202	35.19
32.406 (4)	2.76056	201	15.73	32.411 (3)	2.76014	022	24.15
35.758 (6)	2.50902	103	8.56	33.759 (3)	2.65294	122	16.12
41.25 (1)	2.18674	210	4.80	35.740 (6)	2.51027	131	8.05
43.73 (2)	2.06820	004	2.25	38.978 (4)	2.30889	410	15.82
46.49 (3)	1.95179	212	2.11	41.250 (2)	2.18678	203	12.11
47.874 (3)	1.89854	301	13.63	45. 0 (2)	2.01297	402	2.68
57.92 (4)	1.59084	311	2.12	46.548 (2)	1.94950	303	37.59
58.850 (4)	1.56792	222	13.83	50.303 (5)	1.81240	422	9.75
				53.97 (2)	1.69755	242	3.20

presented (Table 3). The unit cell parameters are found to be changed upon irradiation. The extent of variation in lattice parameters is found to be different in powder and single crystal of the same material (Tables 1, 3). This can be due to the difference in size of single crystal and powdered samples of the same material. Average crystallite size is increased implying aggregation of particle upon irradiation. The marginal increase in cell volume (about 3 %) of irradiated sample (Table 3) suggests the presence of Schottky defects. This will result in a decrease in density which is related to the number of such defects. Moreover a change in lattice parameter suggests, the relaxation around the vacancy is significant [21]. In crystalline systems containing molecular ions irradiation leads to the production of crystal defects and chemical damage. The presence of defects in a crystalline lattice may change both the unit cell size and the physical size of the crystal. The amplitude and phase of the scattered X-rays are determined by the arrangements of atoms in the

Table 3 Lattice parameters of unirradiated and irradiated DMM from PXRD studies

Samples	Lattice constants			Lattice parameters (Å)			Average crystalline size(nm)	Crystal system	Cell volume ($Å^3$)	Density (g/cm^3)
	A	B	C	*a*	*b*	*c*				
Unirradiated	0.00808	0.0085	0.0092	8.5635	8.3316	8.0178	85.4	Orthorhombic	572.05	2.2405
Irradiated	0.0064	0.0085	0.0109	9.6113	8.338	7.3669	138	Orthorhombic	590.37	2.1709

crystal relative to the plane in question. Since atoms have finite size, there is a small path difference between X-rays scattered by electron cloud on opposite sides of atom and this difference increases with increasing 2θ. Since atoms vibrate about a mean position, effective size of atoms will be larger and this leads to a further decrease in scattering power with increase in 2θ. When the crystal is exposed to gamma radiation, atoms in the crystal vibrate more vigorously so that scattering power decreases and hence intensities will be more pronounced. Irradiation can create defects in the crystal. Consequently, the structure factor will vary, and it can cause changes in unit cell parameters. The inter planar distance is related to unit cell dimensions. As a result of increase in vibration of atoms on exposure to gamma radiation, *d*-spacing alters. In addition to structure factor intensity of powder patterns are influenced by polarization factor, multiplicities, and preferred orientations.

Thermal studies

Thermograms of unirradiated and irradiated samples are shown in (Fig. 4). Decomposition of unirradiated and irradiated samples proceeds in two stages. Percentage mass loss during first stage in both the cases corresponds to removal of two moles of water. Also in both the cases ligand pyrolysis occurs during the second stage leading to the formation of manganese dioxide. Phenomenological data with T_i: temperature of inception, T_f: temperature of completion and T_s: peak temperatures along with percentage mass loss for the unirradiated and irradiated samples are presented (Table 4). Thermograms of the unirradiated and irradiated samples are essentially of the same pattern, implying that irradiation has little effect on the decomposition pathway. However, the decomposition is relatively faster in the irradiated samples (Fig. 4). From Table 4, it can also be seen that T_i, T_f and T_s are lowered upon irradiation. These results are in accordance with our previous studies [8, 9]. The decomposition reactivity of crystalline solids depends upon structural and energetic factors associated with the chemical nature of the reactants and products, lattice geometry and defect concentration. As irradiation leads to an increase in defect concentration and subsequent chemical damage, all these factors are modified leading to enhanced rate of decomposition.

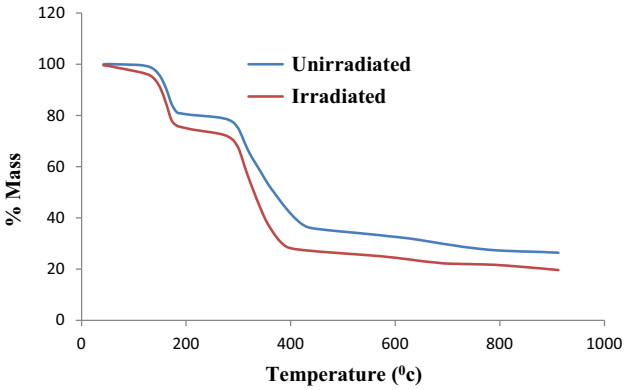

Fig. 4 TG curves of unirradiated and irradiated DMM

Spectral studies

FTIR IR spectra of DMM before and after irradiation are presented in (Fig. 5). Infrared frequencies and their assignments are tabulated (Table 5). The intensity of IR bands of –OH group was found to be increased and the bands in the region 3600–3100 cm^{-1} are found to be broadened in the irradiated sample. The band observed at 3600–3100 cm^{-1} is typical of asymmetric and symmetric stretching vibrations of the –OH group and the broadness of this band points to the existence of hydrogen bonding [22]. It is clear in Fig. 4 that intensity of this band was increased and broadened in the irradiated sample indicating formation of additional –OH and hydrogen bond. Intensity of bands due to carbonyl group is also found to be slightly increased. Factors influencing the intensity of IR peak are dipole moment, concentration of molecules in the sample, transition probability, and so on. Changes in these factors are likely upon irradiation and hence also in the observed intensity. Neither the appearance of new peaks nor the disappearances of the existing peaks are observed upon irradiation.

Photoluminescence spectra in solid state Fluorescence spectra of pure and gamma irradiated DMM in solid state at room temperature are shown in (Fig. 6). The excitation wavelength is 250 nm. The fluorescent spectra of unirradiated samples display four emission bands at wavelengths 345, 389, 414 and 468 nm, while the same of irradiated

Table 4 Thermal decomposition data of unirradiated and irradiated DMM of stage I and II

	Stage I				Stage II			
	T_i	T_f	T_s	% Mass loss	T_i	T_f	T_s	% Mass loss
Unirradiated	384.4	457.27	441.65	19.21	464.2	637.71	582.19	43.44
Irradiated	325.41	450.33	436.45	20.6	460.74	644.65	580.45	44.7

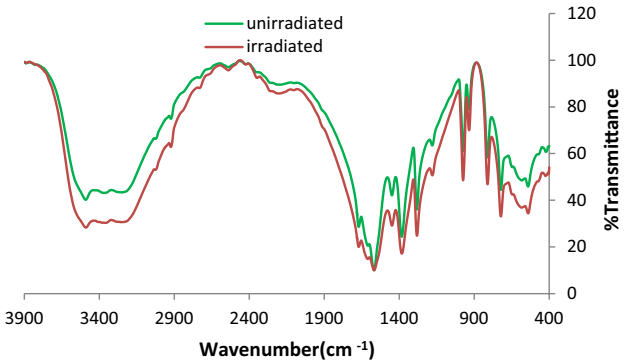

Fig. 5 FTIR spectra of unirradiated and irradiated DMM

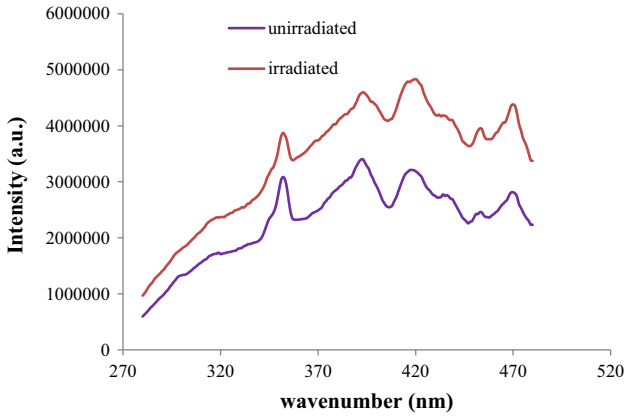

Fig. 6 Emission spectra of unirradiated and irradiated DMM under 250 nm excitation

Table 5 Characteristic bands in the FTIR spectra (400-3895 cm^{-1}) of unirradiated and irradiated DMM

Unirradiated (cm^{-1})	Irradiated (cm^{-1})	Assignments
3100–3500	3100–3500	OH stretching of H_2O
1669.73	1670.83	ν_{as}(OCO)
1567.97	1566.69	ν_{as} (COO^-)
1448.30	1448.03	ν_s(OCO)
1382.84	1382.44	ν_s (COO^-)
1281.69	1281.28	ν_{as} (C–C)
1176.39	1176.39	δ(OH)
973.81	973.82	ν_s (C–C)
933.91	933.90	δ(OH)
810.97	810.89	δ(CH)
721.99	721.86	(COO–) bending

s symmetric stretching, *as* asymmetric stretching, δ deformation

sample are at 351, 391, 415 and 468 nm respectively. In the unirradiated sample maximum emission band is observed at 389 nm while that in irradiated sample, it appears at 415 nm. All the bands in (Fig. 6) can be assigned to ligand to metal charge transfer. These are allowed transitions and hence they are very intense. PL intensity is found to be increased and the band positions are found to be slightly shifted upon irradiation. The maximum increase (56 %) is observed at 414 nm. Two factors which influence the intensities are transition probability and population of the state from which transition occurs. Transition probability is expressed in terms of selection rules. Charge transfer bands are allowed and therefore are generally intense. Since the intensities of emission bands of irradiated sample are higher, it can be concluded that the population in the excited state is greater for the irradiated sample. The increase in population of excited state may be related to the crystal defects and radiation damage. The enhancement in the PL intensity of the irradiated samples may also be due to the induced distortions in the crystal lattice of DMM as evidenced from PXRD studies. Enhancement of PL intensity upon irradiation has been reported earlier [11, 12]. The enhancement in the PL intensity of the irradiated samples of spinel ferrite has been attributed to the induced distortions in the crystal lattice [12]. The observed bathochromic shift (345–351 and 389–391 nm) is important, because, disruption of the coordination environment in metal complexes induces such a shift depending on the amount of disruption. So, this can be an evidence of a structural change which may be arising from the disruption of the coordinated water molecules. Hence structural changes as a result of irradiation cannot be ruled out because there are changes in position of bands.

UV–Vis spectrum in solid state UV visible spectrum of DMM before and after irradiation is presented in (Fig. 7). In UV spectra of unirradiated and irradiated DMM peaks characteristics of Mn(II) were observed. Since all *d–d* transitions are forbidden for Mn(II) in an octahedral field, all the bands are of weak intensity. The charge transfer band, which is allowed, is observed around 240 nm. The intra ligand π–π^* transition due to carbonyl group also appears in the range 210–240 nm. The intensity of these bands is lowered in the irradiated sample. The

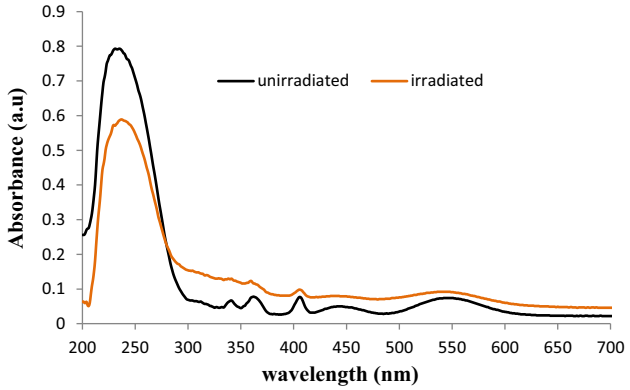

Fig. 7 UV–Vis spectra of unirradiated and irradiated DMM

lowering of intensity of charge transfer band can be attributed to irradiation damage of the ligand. This observation is in agreement with our earlier studies [2, 4, 5]. Also, the bands due to *d–d* transition have broadened in the UV spectrum of irradiated sample. This is possible only if the field strength fluctuates over a significant range of energy [2]. The intensity of these bands has slightly increased and they tend to coalesce. Irradiation can cause perturbation of energy levels as well as deformity in the molecule. Under these circumstances the selection rules may be violated and the *d–d* transitions gain some intensity due to perturbation of energy levels.

AFM Atomic force microscopy was performed to examine the surface morphology and to measure roughness values for unirradiated and irradiated DMM (600 kGy). Figure 8a, b shows the two and three dimensional topographic scan of the unirradiated and irradiated samples respectively. Unirradiated DMM shows the presence of nano hillock with average diameter 119 nm and height in

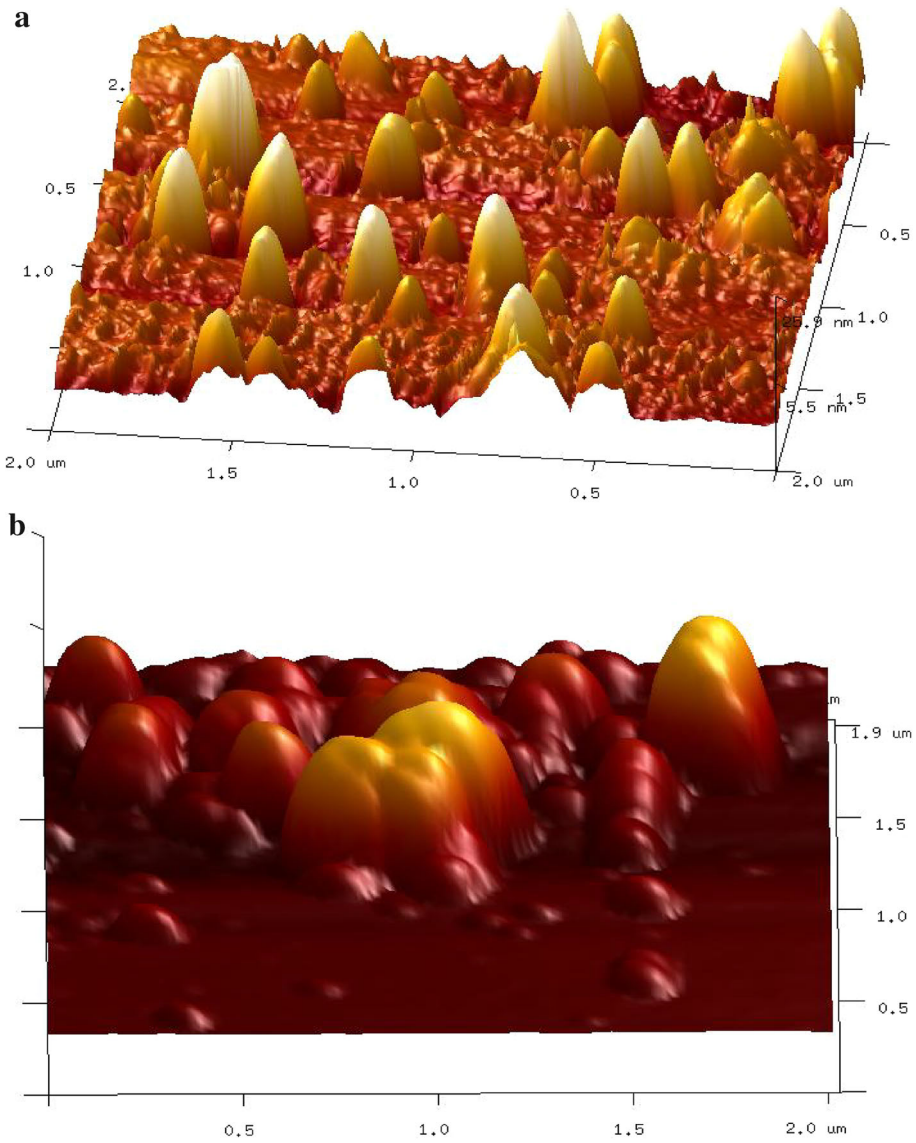

Fig. 8 **a** Three dimensional view of AFM micrograph of unirradiated DMM. **b** Three dimensional view of AFM micrograph of irradiated DMM

the range 10–32 nm, the roughness being 3.36 nm. In the irradiated samples aggregation of particles form the appearance of very huge hump (protrusion) (Fig. 8b). The average diameter is found to be 280 nm and height in the range of 46–132 nm with roughness of 18.5 nm. Results reveal that gamma irradiated surface was rougher compared to the unirradiated sample surface. It can be noted from (Fig. 8b) that significant disturbance is created in the irradiated DMM. It is well known that solid state irradiation of molecular crystals leads to crystal defects and chemical damage. The major fragments of radiolysis of malonic acid are carbon dioxide and acetic acid and that of water are radical species ($H\cdot$,$\cdot OH$, e^-) and molecular products (H_2, H_2O_2) [23, 24]. Presence of these fragments can be expected in irradiated DMM as well. Gaseous products like carbon dioxide and hydrogen diffuse throughout the area as bubbles, thus increasing the internal pressure leading to surface deformation and subsequent formation of very huge hump with an aggregation of large amount of material. The transition from nano hillock to larger humps occurs due to diffusion, transformation and aggregation of defects [25]. The increase in the roughness may be due to the change in crosslinking density and degradation of the polymeric chain surface [26].

Conclusions

From single crystal studies it is seen that the complex DMM crystallizes in orthorhombic space group $Pca2_1$ and is having a polymeric structure. Irradiation does not change the geometry of the system and changes in lattice parameters are negligible. From PXRD studies also it was observed that the orthorhombic geometry was retained upon irradiation but the changes in lattice parameters are significant. Effect of irradiation on single crystal and PXRD are different. Thermo grams of unirradiated and irradiated samples are found to be similar but the irradiated sample shows an enhanced rate of decomposition. Spectral studies indicated structural changes after irradiation. Photoluminescent property is found to be enhanced by irradiation. AFM studies suggested surface deformation and transition from nano hillock to larger humps upon irradiation.

Supplementary material

CCDC 1001534 contains the supplementary crystallographic data for this paper. These data can be obtained free of charge from The Cambridge Crystallographic Data Centre via deposit@ccdc.cam.ac.uk or from the Cambridge Crystallographic Data Centre, 12 Union Road, Cambridge CB2 1EZ, UK; fax:(+44)1223336033.

Acknowledgments The authors are thankful to the Pondicherry Central Instrument Facility for ^{60}Co gamma irradiation, SAIF, Cochin University of Science and Technology, Kochi for analytical facilities. We are grateful to Dr. Shibu M. Eapen, SAIF, CUSAT, Kochi, India for providing single crystal X-ray diffraction data. One of us, ISS, is grateful to the University of Kerala for the award of a fellowship.

References

1. Al-Resayes SI (2010) Arabian J Chem 3:191–194
2. Jayashri TA, Krishnan G (2008) J Radioanal Nucl Chem 277:693–697
3. Sekkina MMA, El-Boraey HA, Aly SA (2014) J Radioanal Nucl Chem 300:867–872
4. Krishnan G, Jayashri TA, Geetha Devi K (2009) Radiat Phys Chem 78:184–190
5. Krishnan G, Jayashri TA, Sudha P (2009) Radiat Phys Chem 78:933–938
6. Fares S (2012) Nat Sci 4:499–507
7. Ahamad T, Alshehri SM (2014) Arab J Chem 7:1140–1147
8. Jayashri TA, Krishnan G, Viji K (2014) J Radioanal Nucl Chem 302:1021–1026
9. Jayashri TA, Krishnan G, Rema Rani N (2014) Radiat Eff Defects Solids 169:1019–1030
10. Yildirim I, Karabulut B, Bozkurt E, Koksal F (2009) Radiat Phys Chem 78:165–167
11. Gokul Raj S, Ramesh Kumar G (2011) Int J Curr Sci 1:91–97
12. Imam NG, Hashhash A (2014) Nucl Instrum Methods Phys Res A 767:353–358
13. Ruiz-Perez C, Rodriguez-Martin Y, Hernandez-Molina M, Delgado FS, Pasan J, Sanchiz J, Lloret F, Julve M (2003) Polyhedron 22:2111–2123
14. Pasan J, Delgado FS, Rodriguez-Martin Y, Hernandez-Molina M, Ruiz-Perez C, Sanchiz J, Lloret F, Julve M (2003) Polyhedron 22:2143–2153
15. Altomare A, Cascarano M, Giacovazzo C, Guagliardi A (1993) J Appl Crystallogr 26:343–350
16. Scheldrick GM (2008) Acta Crystallogr A 64:112–114
17. Brandenburg K (2012) Diamond Version 3.2i, Crystal Impact GbR, Bonn
18. Lis T, Matuszewski J (1979) Acta cryst. 35:2212–2214
19. Lipson H, Steeple H (1979) Interpretation of X-ray powder diffraction patterns. Macmillan, London
20. West AR (1984) Solid state chemistry and its applications. Wiley, New York
21. Henderson B (1972) Defects in crystalline solids. Edward Arnold, London
22. Mathew Varghese, Joseph Jochan, Jacob Sabu, Abram KE (2010) Bull Mater Sci 33:433–437
23. Hosaka A, Sugimori A, Genka T, Tsuchihashi G (1967) Bull Chem Soc Jpn 40:1799–1803
24. Sophie Le Caër (2011) Water. 3:235–253
25. Rafique MS, Bashir S, Husinsky W, Hobro A, Lendl B (2012) Appl Surf Sci 258:3178–3183
26. Khayet M (2004) Appl Surf Sci 238:269–272